

# CRISPR-Cas9 knockout of DGK $\alpha/\zeta$ improves the anti-tumor activities of TAG-72 CAR-T cells in ovarian cancer

Vera J. Evtimov,<sup>1,2,5</sup> Nhu-Y N. Nguyen,<sup>1,2,5</sup> Maree V. Hammett,<sup>1,2,5</sup> Aleta Pupovac,<sup>1,2</sup> Peter J. Hudson,<sup>1,2</sup> Junli Zhuang,<sup>1,2</sup> Jae Young Lee,<sup>3</sup> Seokjoong Kim,<sup>3</sup> Alan O. Trounson,<sup>1,2</sup> Richard L. Boyd,<sup>1,2</sup> and Runzhe Shu<sup>1,4</sup>

<sup>1</sup>Cartherics Pty Ltd, Notting Hill, VIC 3168, Australia; <sup>2</sup>Australian Regenerative Medicine Institute, Monash University, Clayton, VIC 3168, Australia; <sup>3</sup>ToolGen Inc., Seoul 153783, South Korea

**High recurrence and chemoresistance in solid tumors, like ovarian cancer, stress the need for new therapies. Chimeric antigen receptor (CAR)-T cells show promise but face challenges due to tumor heterogeneity and immune suppression in the tumor microenvironment (TME). Thus, novel approaches are needed to further enhance the efficacy of CAR-T cell therapies. In T cell therapies, inhibiting checkpoint molecules is crucial for overcoming exhaustion and boosting anti-tumor activity. Additionally, prioritizing safety by engineering cells to target markers absent on normal healthy cells reduces off-target risks. We targeted tumor-associated glycoprotein 72 (TAG-72), an oncofetal antigen highly expressed in adenocarcinomas like ovarian cancer, by engineering TAG-72 CAR-T cells and used CRISPR-Cas9 to knock out the T cell-inhibitory enzymes diacylglycerol kinase (DGK)  $\alpha$  and  $\zeta$ . DGK $\alpha/\zeta$  knockout (KO) did not impact CAR-T cell viability or phenotype. These cells selectively killed TAG-72-expressing cancer cells *in vitro* and ablated established tumors *in vivo* for up to 100 days, whereas non-deleted control TAG-72 CAR-T cells showed tumor relapse around 40 days. These findings highlight the potential of CRISPR-induced DGK $\alpha/\zeta$  KO to enhance CAR-T cell efficacy against solid tumors such as ovarian cancer, offering a promising avenue for improved cancer therapies.**

## INTRODUCTION

Chimeric antigen receptor (CAR)-T cell therapies have shown significant clinical success in treating chemotherapy-resistant or refractory B cell malignancies, resulting in their approval by the US Food and Drug Administration and revolutionizing the field of cancer immunotherapy.<sup>1</sup> Despite this, however, documented efficacy against solid tumors is limited. This is attributed to tumor antigen heterogeneity, difficulties trafficking to and infiltrating the tumor, and the immune-suppressive tumor microenvironment (TME).<sup>2</sup> Given the many and complex layers of immune-suppressive mechanisms induced by a range of different immune cell checkpoint molecules and soluble factors in the TME, novel approaches to combination therapies for solid tumors are required. Knockout (KO) of regulators in the signaling pathways that restrict T cell cytotoxicity and/or

expansion can aid in augmenting anti-tumor T cell function.<sup>3</sup> Genome editing tools such as transcription activator-like effector nucleases (TALENs) and clustered regulatory interspaced short palindromic repeats (CRISPR)-Cas are being used to manipulate cells for cancer treatment and other diseases. In pre-clinical studies, CRISPR<sup>4</sup> or TALEN<sup>5</sup> inactivation of PD-1 in T cells improves *in vitro* and *in vivo* tumor clearance and T cell persistence. Multiple clinical trials are also assessing clinical outcomes of CAR-T cells with CRISPR KO of checkpoint molecules in a variety of cancer indications.<sup>6–8</sup>

Diacylglycerol kinases (DGKs) are lipid kinases expressed in numerous cell types, including T cells. DGKs reduce the intracellular mediator diacylglycerol by catalyzing its phosphorylation to phosphatidic acid (PA), thereby negatively regulating T cell function.<sup>9–11</sup> DGK $\alpha$  and DGK $\zeta$  are the two predominant DGK isoforms expressed in T cells. The DGK $\alpha$  isoform in particular is established as an inhibitory immune checkpoint.<sup>10–13</sup> CAR-T cells undergo a rapid loss of functional activity associated with the upregulation of DGK and inhibitory receptors upon tumor killing, leading to limited therapeutic efficacy.<sup>14</sup> Other pre-clinical studies also show that deleting DGK $\alpha$  and DGK $\zeta$ , either individually or simultaneously, improves T cell function. In murine models, adoptive transfer of DGK $\alpha$  or DGK $\zeta$  KO CAR-T cells had similar efficacy against murine mesothelioma.<sup>13,15</sup> Furthermore, a pre-clinical study showed that disruption of either DGK isoform or deletion of both DGK $\alpha$  and DGK $\zeta$  potentiates the anti-tumor function of human CAR-T cells against

Received 30 August 2024; accepted 28 February 2025;  
<https://doi.org/10.1016/j.omton.2025.200962>

<sup>4</sup>Present address: Shunxi Bio-Pharmaceutical Technology Co., Ltd., Hangzhou 310000, China

<sup>5</sup>These authors contributed equally

**Correspondence:** Vera J. Evtimov, Cartherics Pty Ltd, Notting Hill, VIC 3168, Australia.

**E-mail:** vera.evtimov@monash.edu

**Correspondence:** Runzhe Shu, Cartherics Pty Ltd, Notting Hill, VIC 3168, Australia.

**E-mail:** runzhe.shu@shunxibio.com



glioblastoma, rendering them more resilient upon repeated tumor exposure.<sup>16</sup>

Metabolite levels are altered in cancer cells, and controlling these alterations may be exploited for improving cancer therapy.<sup>17</sup> In this regard, PA, produced by the action of DGK, acts as a critical signaling effector in cisplatin resistance of ovarian cancer.<sup>18</sup> Ovarian cancer is a leading cause of cancer-related deaths among women, and new therapies are needed to curb its high recurrence rate and resistance to chemotherapy.<sup>19,20</sup> Tumor-associated glycoprotein 72 (TAG-72) is overexpressed on the surface membrane of ovarian cancer and other adenocarcinomas.<sup>21–24</sup> TAG-72 expression has been associated with all ovarian cancer subtypes and is directly correlated with poorer prognoses.<sup>25,26</sup> Previously, we and others have shown that CAR-T cells targeting TAG-72 can kill ovarian cancer cells *in vitro* and *in vivo*.<sup>27,28</sup> We thus hypothesized that deletion of the DGK enzymes would improve the tumor killing ability of TAG-72 CAR-T cells. Accordingly, we used CRISPR-Cas9 editing to knock out the DGK $\alpha$  and DGK $\zeta$  isoforms in TAG-72-targeting CAR-T cells and assessed their capacity to eradicate ovarian cancer cells *in vitro* and *in vivo*.

## RESULTS

### Characterization of TAG-72 CAR/DGK $\alpha/\zeta$ KO T cells

The generation of TAG-72 CAR/DGK $\alpha/\zeta$  KO T cells is a two-step gene-editing process (Figure 1A). Human T cells were transduced with a second-generation CAR containing an anti-TAG-72-specific scFv (single-chain variable fragment) coupled to a CD8 hinge, a 4-1BB intracellular co-stimulatory domain linked to a CD3 $\zeta$  signaling domain, and an enhanced green fluorescent protein (EGFP) reporter, as described previously<sup>27</sup> (Figure 1B). Significant CAR expression was observed in human T cells 11–13 days post transduction (Figure 1C). DGK $\alpha$  and DGK $\zeta$  guide ribonucleic acid (gRNA) induced insertions or deletions (indels) and KO at high efficiency in CAR-T cells, respectively (Figure 1D). Specifically, the DGK $\alpha$  gRNA showed a total indel percentage of 87.33%  $\pm$  9.07% with a KO efficiency of 48.00%  $\pm$  16.82%. The DGK $\zeta$  gRNA exhibited a total indel percentage of 93.33%  $\pm$  2.52% with a KO efficiency of 75.33%  $\pm$  2.08%. These results indicate that both DGK $\alpha$  and DGK $\zeta$  gRNAs are highly effective in inducing indels and achieving substantial KO efficiencies in CAR-T cells. Additionally, deletion of DGK $\alpha$  and DGK $\zeta$  genes in CAR-T cells led to the reduction of the DGK $\alpha$  and DGK $\zeta$  proteins (Figure 1E). To further characterize TAG-72 CAR/DGK $\alpha/\zeta$  KO T cells, we analyzed the prevalent T cell subset and compared the expression of T cell exhaustion markers to TAG-72 CAR-T cells and unedited T cells. The proportions of T cell subsets (CD8<sup>+</sup>, double-positive, CD4<sup>+</sup>, double-negative) remained uniform, with CD4<sup>+</sup> and effector memory (CCR7<sup>−</sup>/CD45RO<sup>+</sup>) cells being the prevalent phenotypes (Figure 1F). All exhaustion markers (TIM-3 [T cell immunoglobulin and mucin-domain containing 3], PD-1 [programmed cell death protein 1], and LAG3 [lymphocyte-activation gene 3]) were also expressed at similar levels in TAG-72 CAR/DGK $\alpha/\zeta$  KO T cells and controls (Figure 1F).

### TAG-72 CAR/DGK $\alpha/\zeta$ KO T cells proliferate and exhibit potent cytotoxicity *in vitro*

The deletion of DGK genes did not impact the overall viability or proliferative potential of CAR-T cells (Figures 2A and 2B). Following electroporation on day 5, TAG-72 CAR/DGK $\alpha/\zeta$  KO T cells demonstrated a slight reduction in viability (Figure 2A) and lag in expansion (Figure 2B), which were both attributed to the electroporation process. Following 9 days of expansion, however, both viability and total cell number were comparable to TAG-72 CAR-T cell controls. These data suggest that these gene deletions should not impact the ability to produce sufficient cell numbers for a clinical product. The cytotoxic activity of TAG-72 CAR/DGK $\alpha/\zeta$  KO T cells was subsequently assessed *in vitro* using the real-time cell analysis system, xCELLigence. TAG-72 CAR/DGK $\alpha/\zeta$  KO T cells selectively killed the TAG-72<sup>mid</sup> ovarian cancer cell target (OVCAR-3 cells; Figure 2C) but not the TAG-72<sup>low</sup> ovarian cancer cell target (MES-OV) (Figure 2D). These results indicated that deletion of DGK did not impact the *in vitro* cytotoxicity and specificity of TAG-72 CAR/DGK $\alpha/\zeta$  KO T cells compared to TAG-72 CAR-T cell controls.

### Cytokine profile of CAR-T and ovarian cancer cell co-cultures

We evaluated the amounts of secreted cytokines, chemokines, and growth factors in the supernatants following culture of either unedited T cells, TAG-72 CAR-T cells, or TAG-72 CAR/DGK $\alpha/\zeta$  KO T cells with target cells.

### Pro-inflammatory and regulatory cytokines

The levels of interleukin (IL)-1 $\beta$  were significantly higher in the supernatants from TAG-72 CAR-T cells compared to unedited T cells. This response was further enhanced when target cells were co-cultured with TAG-72 CAR/DGK $\alpha/\zeta$  KO T cells, suggesting that DGK deletion may amplify the IL-1 $\beta$  response (Figure 3A). Elevated levels of IL-9 and IL-15 were observed after treatment with TAG-72 CAR/DGK $\alpha/\zeta$  KO T cells; increased IL-15 levels were also noted with TAG-72 CAR-T cells. However, there was no significant difference in IL-9 and IL-15 levels between TAG-72 CAR-T cells and TAG-72 CAR/DGK $\alpha/\zeta$  KO T cells, suggesting that DGK deletion does not affect IL-9 or IL-15 production (Figure 3A). TAG-72 CAR/DGK $\alpha/\zeta$  KO T cells induced a significant increase in granulocyte-macrophage colony-stimulating factor (GM-CSF) levels compared to unedited T cells and TAG-72 CAR-T cells, indicating that DGK deletion may enhance GM-CSF production. TAG-72 CAR-T cells alone did not significantly alter GM-CSF levels (Figure 3A). The supernatants from TAG-72 CAR-T cells and TAG-72 CAR/DGK $\alpha/\zeta$  KO T cells exhibited higher levels of monocyte chemoattractant protein-1 (MCP-1) compared to unedited T cells, with no significant difference between the two CAR-T cell types, implying that DGK deletion does not influence MCP-1 production (Figure 3A). TAG-72 CAR/DGK $\alpha/\zeta$  KO T cells also increased tumor necrosis factor alpha (TNF $\alpha$ ) levels compared to unedited T cells and TAG-72 CAR-T cells, while TAG-72 CAR-T cells alone did not significantly affect TNF $\alpha$  levels, suggesting that the DGK deletion may enhance TNF $\alpha$  production (Figure 3A). IL-8 levels were slightly elevated in the presence of TAG-72 CAR/DGK $\alpha/\zeta$  KO T cells compared to unedited T cells,

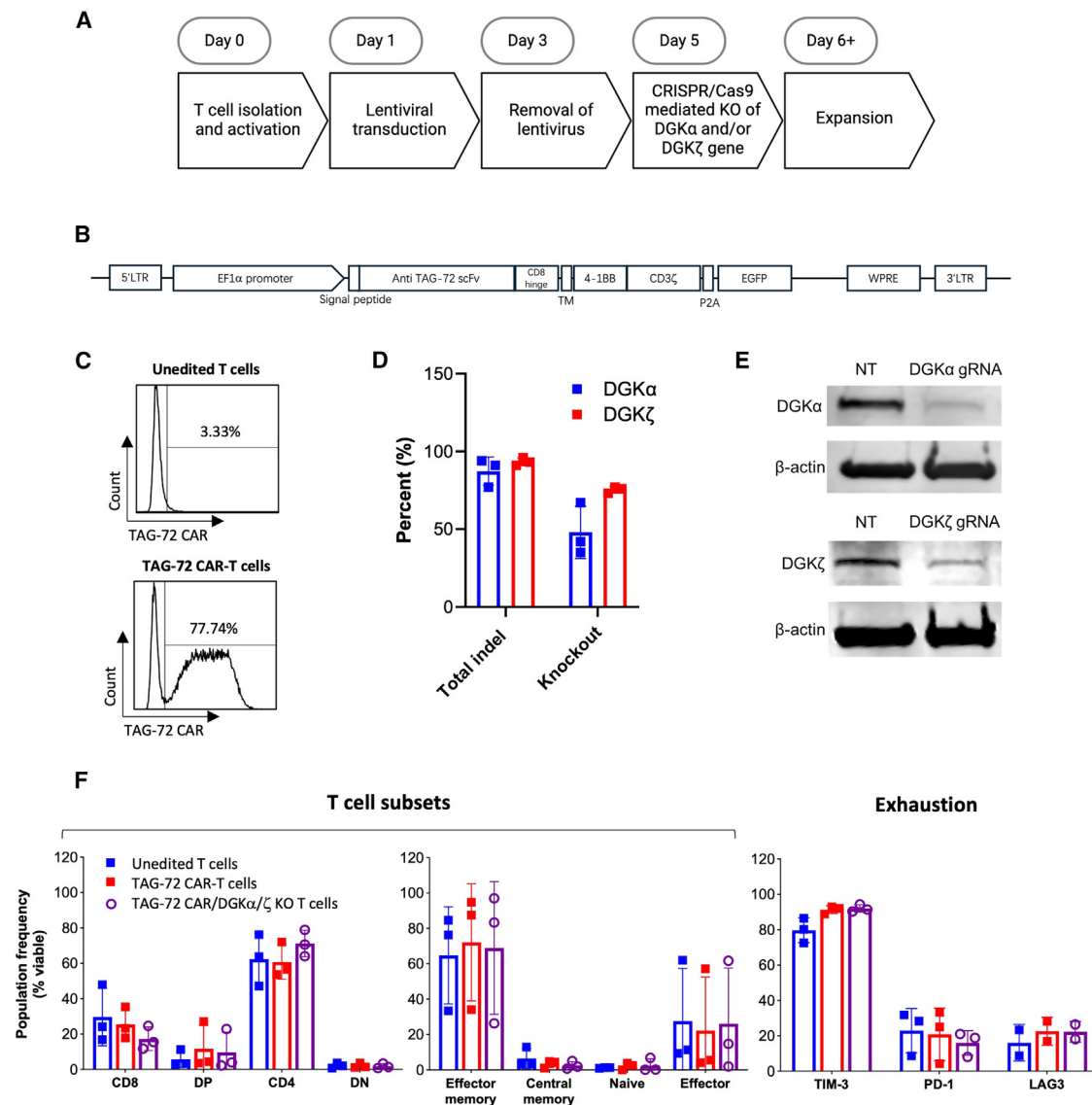


**Figure 1. Characterization of TAG-72 CAR/DGKα/ζ KO T cells**

(A) Overview of the process used to produce CAR-T cells. (B) Schematic of the lentiviral expression cassette containing an anti-TAG-72-specific scFv, CD8 hinge domain, and 4-1BB intracellular co-stimulatory domain linked to a CD3ζ signaling domain. (C) Transduction efficiency of the TAG-72 CAR was assessed using flow cytometry at least 11 days after transduction. Unedited T cells were included as a control. Representative of 3 independent experiments. (D) Frequency of total indels and KO (proportion of indels that indicate frameshift mutations) of DGKα and DGKζ genes in the pooled gene-edited CAR-T cells as assessed by ICE analysis ( $n = 3$  independent donors). (E) Western blots of DGKα and DGKζ protein in TAG-72 CAR/DGKα/ζ KO CAR-T cell lysates and unedited control T cells (NT). β-actin was used as a loading control. (F) Flow cytometry analysis was performed to examine the common T cell-associated surface markers CD4 and CD8 and effector memory (CCR7<sup>+</sup>/CD45RO<sup>+</sup>), central memory (CCR7<sup>+</sup>/CD45RO<sup>+</sup>), naive (CCR7<sup>+</sup>/CD45RO<sup>-</sup>), and effector (CCR7<sup>-</sup>/CD45RO<sup>-</sup>) cell subsets and exhaustion markers (as indicated). Frequencies are presented as a proportion of viable cells ( $n = 3-4$  independent donors). A Kruskal-Wallis non-parametric test confirmed no significant differences between groups.

whereas TAG-72 CAR-T cells did not significantly alter IL-8 levels. There was no significant difference between TAG-72 CAR-T and TAG-72 CAR/DGKα/ζ KO T cells in terms of IL-8 production, indicating no impact of DGK deletion on this cytokine. No altered levels of interferon γ (IFNγ), IL-2, IL-7, IL-17A, IL-6, or IL-12(p70) were observed (Figure 3A).

#### Anti-inflammatory cytokines

The levels of IL-1 receptor antagonist (IL-1Ra) were significantly increased in the supernatants from both TAG-72 CAR-T cells and TAG-72 CAR/DGKα/ζ KO T cells compared to unedited T cells, with a more pronounced increase observed in the presence of the latter, suggesting that DGK deletion might enhance the IL-1Ra

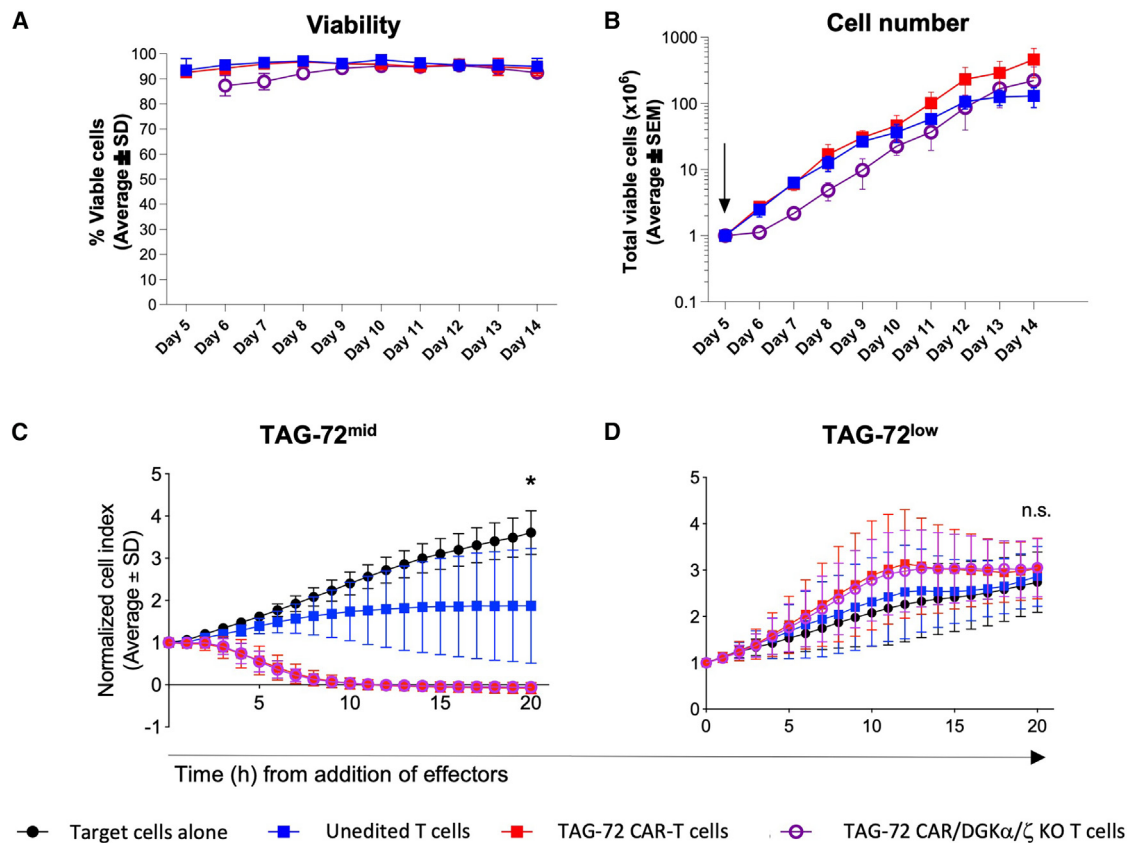


**Figure 2. TAG-72 CAR/DGK $\alpha$ / $\zeta$  KO T cells demonstrate proliferation and potent *in vitro* tumor cell killing capability**

(A and B) Following T cell activation, transduction, and electroporation, cells were maintained in T cell expansion medium; (A) viability and (B) cell number are shown. Data are normalized to the time of electroporation ( $\downarrow$ ). (C) TAG-72<sup>mid</sup> (OVCAR-3) and (D) TAG-72<sup>low</sup> (MES-OV) target cells were co-cultured with unedited T cells, TAG-72 CAR-T cells, or TAG-72 CAR/DGK $\alpha$ / $\zeta$  KO T cells at an E:T ratio of 5:1, and the response was monitored in real time using xCELLigence, where a decrease in the normalized CI is indicative of target cell death relative to target cells alone (black). Data are pooled from independent experiments ( $n = 4$  biological replicates). A one-way ANOVA was used to determine statistical significance. \* $p \leq 0.05$ . n.s., not significant.

response (Figure 3B). IL-4 levels were slightly higher following TAG-72 CAR/DGK $\alpha$ / $\zeta$  KO T cell treatment compared to unedited T cells, but there was no significant difference between TAG-72 CAR-T cells and the other groups. No elevated levels of IL-10 or IL-13 were observed (Figure 3B).

#### Chemotactic factors

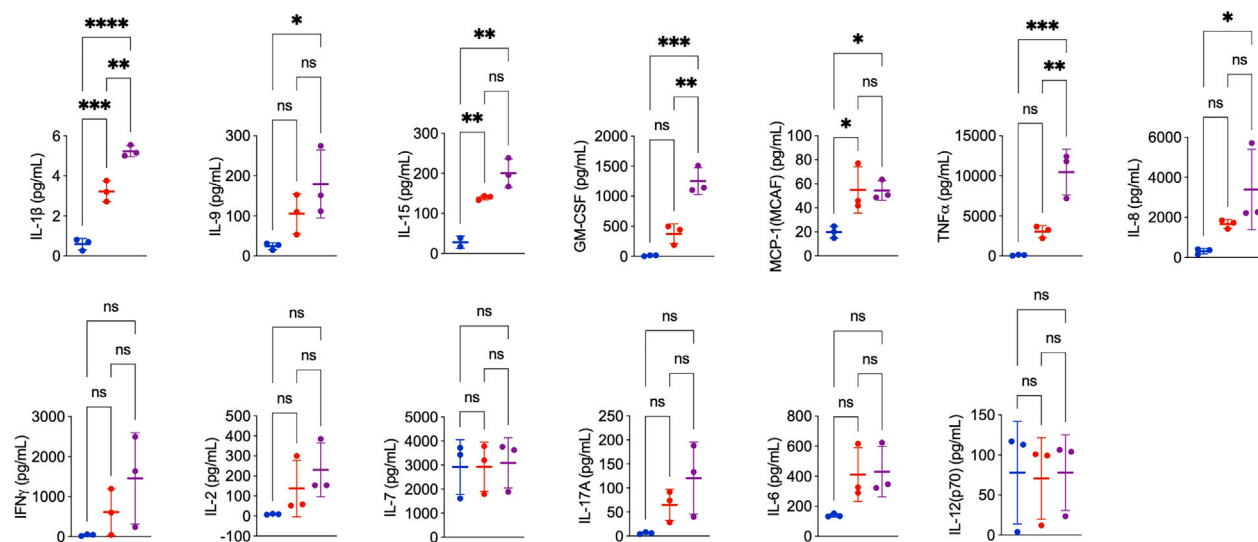
TAG-72 CAR/DGK $\alpha$ / $\zeta$  KO T cells had significantly increased levels of the chemokines macrophage inflammatory protein (MIP)-1 $\alpha$  and MIP-1 $\beta$ , but no significant increases were observed with TAG-72 CAR-T cells (Figure 3C). This indicates and aligns with the finding that DGK deletion may contribute to the recruitment and activation of various immune cells.<sup>29</sup> No elevated levels of IP-10 were observed. RANTES levels were slightly increased by TAG-72 CAR/DGK $\alpha$ / $\zeta$  KO T cells compared to the control, suggesting a potential role in enhancing immune cell recruitment and activation (Figure 3C). Both TAG-72 CAR-T cells and TAG-72 CAR/DGK $\alpha$ / $\zeta$  KO T cells increased vascular endothelial growth factor (VEGF) levels compared to unedited T cells, indicating a potential enhancement of angiogen-

esis.<sup>30</sup> The lack of a significant difference between TAG-72 CAR-T and TAG-72 CAR/DGK $\alpha$ / $\zeta$  KO T cells suggests that DGK deletion does not alter VEGF production. Eotaxin levels were elevated by both TAG-72 CAR-T cells and TAG-72 CAR/DGK $\alpha$ / $\zeta$  KO T cells compared to unedited T cells, with a slight additional increase observed with TAG-72 CAR/DGK $\alpha$ / $\zeta$  KO T cells (Figure 3C). This could suggest an enhanced ability to attract eosinophils, which are important in inflammatory responses and may play a role in anti-tumor activity.<sup>31</sup>

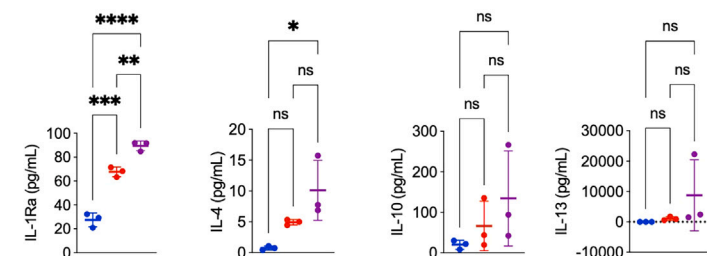
#### Growth factors

Platelet-derived growth factor BB (PDGF-BB), basic fibroblast growth factor (FGF basic), and granulocyte colony-stimulating factor (G-CSF) were significantly elevated by both TAG-72 CAR-T cells and TAG-72 CAR/DGK $\alpha$ / $\zeta$  KO T cells compared to unedited T cells (Figure 3D). Notably, all growth factors were induced at higher levels by TAG-72 CAR/DGK $\alpha$ / $\zeta$  KO T cells than TAG-72 CAR-T cells, suggesting that the DGK deletion may enhance their production. The factors may contribute to cell proliferation and tissue remodeling.<sup>32</sup>

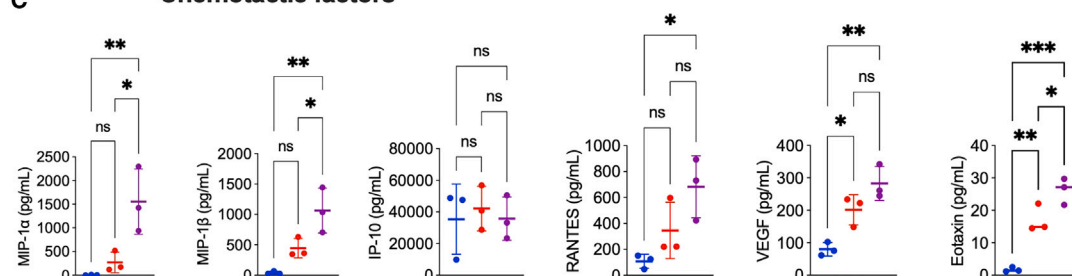
## A Pro-inflammatory / regulatory cytokines



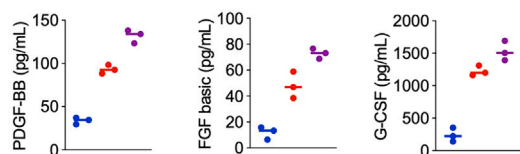
## B Anti-inflammatory cytokines



## C Chemotactic factors



## D Growth factors



(legend on next page)



### TAG-72 CAR/DGK $\alpha$ / $\zeta$ KO T cells ablate established tumors *in vivo*

To assess the anti-tumor activity of TAG-72 CAR/DGK $\alpha$ / $\zeta$  KO T cells *in vivo*, an ovarian cancer non-obese diabetic/severe combined immunodeficiency gamma (NSG) xenograft mouse model was generated by subcutaneous (s.c.) injection of TAG-72<sup>mid</sup> OVCAR-3 cells into NSG mice. Xenograft animals were allowed to establish a palpable tumor mass prior to injection with T cells (Figure 4A). Mice treated with TAG-72 CAR-T cells initially showed a robust anti-tumor response but began to relapse by day 40. Similarly, mice treated with single DGK KO CAR-T cells, either TAG-72 CAR/DGK $\alpha$  or TAG-72 CAR/DGK $\zeta$  T cells, also exhibited strong anti-tumor responses, with a slightly delayed relapse around day 50. In contrast, mice treated with TAG-72 CAR/DGK $\alpha$ / $\zeta$  KO T cells maintained tumor eradication up to the experiment end (100 days; Figure 4B), and correspondingly Kaplan-Meier analysis of these mice against all other groups showed a survival advantage (Figure 4C). Following this time, immunohistochemistry (IHC) analysis of any remaining tumors revealed high levels of human CD3<sup>+</sup> T cells at the tumor site in mice treated with TAG-72 CAR/DGK $\alpha$ / $\zeta$  KO T cells. Conversely, mice treated with unedited T cells exhibited no CD3<sup>+</sup> cells at their experimental endpoint (30 days, tumor volume > 1,000 mm<sup>3</sup>) and significant tumor growth (Figure 4D), highlighting the efficacy and durability of the TAG-72 CAR/DGK $\alpha$ / $\zeta$  KO T cells in tumor eradication and persistence.

## DISCUSSION

In this study, we utilized CRISPR-Cas9 to successfully delete DGK $\alpha$  and DGK $\zeta$ , creating TAG-72 CAR/DGK $\alpha$ / $\zeta$  KO T cells. These cells retained viability and proliferation capacity comparable to those of TAG-72 CAR-T controls. Notably, the distribution of T cell subsets, characterized by a predominance of CD4<sup>+</sup> cells and effector memory cells, remained unchanged following DGK $\alpha$ / $\zeta$  KO. Furthermore, the expression levels of T cell exhaustion markers and *in vitro* killing specificity were similar to those of control groups. These similarities are key, as they confirm the validity of advancing these cells into clinical product development. The capacity of TAG-72 CAR/DGK $\alpha$ / $\zeta$  KO cells to eliminate tumor cells *in vitro*, eradicate established tumors *in vivo*, and prevent their recurrence for up to 100 days underscores their potential as a therapeutic option for TAG-72<sup>+</sup> cancers. While there are clearly advantages in deleting both DGK $\alpha$  and DGK $\zeta$  genes, the safety of administration of these gene-edited CAR-T cells needs to be carefully assessed. Pre-clinical studies, such as cytokine-independent proliferation assays or soft agar colony formation, could be implemented to evaluate the potential tumorigenicity of these cells. In addition, as gene editing may lead to off-target oncogenic events, it is essential to perform genomic surveillance, such as GUIDE-Seq, whole-genome sequencing, and/or chromosomal translocation anal-

ysis. In the clinical setting, these gene-edited CAR-T cells can be monitored by regular blood sampling, allowing for the detection of renewed proliferation of CAR-T cells and an understanding of their persistence.

In our current study and previous work,<sup>27</sup> we demonstrated the effectiveness of TAG-72 CAR-T cells against ovarian cancer in both *in vitro* and *in vivo* settings. The first clinical trial of a TAG-72 CAR-T product used a first-generation CAR construct for treating patients with colorectal cancer.<sup>33</sup> These cells were evaluated for safety but demonstrated limited efficacy and potential for immunogenicity risks. The construct was designed using the TAG-72 scFv, derived from a humanized CC49 antibody. It was observed that the affinity of this humanized scFv was decreased, likely due to numerous amino acid mutations introduced during humanization. Such a decrease in affinity may have influenced the therapeutic efficacy of the antibody. Conversely, the study here and our previous study utilized a deimmunized murine version of the anti-TAG-72 antibody, which has been used most recently in clinical biodistribution trials.<sup>24</sup> These trials demonstrated high specificity for adenocarcinomas, high affinity for the target, and, crucially, low immunogenicity.<sup>24</sup> This highlights an advantage of using deimmunized murine versions for CAR-T therapy, promoting improved efficacy and safety in treating TAG-72<sup>+</sup> cancers.

DGK $\alpha$  and DGK $\zeta$  are two isoforms within the DGK enzyme family, pivotal for converting diacylglycerol (DAG) to PA, impacting various aspects of T cell biology, such as development, proliferation and function.<sup>34</sup> These isoforms act as a regulatory mechanism in T cells, dampening DAG-mediated signals to prevent excessive immune cell activation after T cell receptor (TCR) stimulation. This regulation prevents T cells from entering a hyporesponsive state characterized by diminished DAG-mediated signaling and elevated DGK $\alpha$  and DGK $\zeta$  levels, establishing these enzymes as critical checkpoints in the immune response.<sup>34</sup> Deleting DGK $\alpha$  or DGK $\zeta$  enhances TCR-induced cytokine production, T cell proliferation, and the CD8<sup>+</sup> T cell anti-tumor response, with both isoforms uniquely contributing to T cell function within the immune-suppressive TME. Complete deletion of both DGK $\alpha$  and DGK $\zeta$  isoforms is essential to maximize anti-tumor immunity, highlighting their distinct roles.<sup>16,35,36</sup> Thus, targeting DGK is a promising approach for immunotherapy. However, challenges still hinder its application; for example, DGKs, being intracellular, cannot be targeted using antibodies, and specific inhibitors for DGK $\alpha$  or DGK $\zeta$  are also lacking, with existing ones affecting multiple DGK isotypes, risking unintended effects.<sup>36</sup> In contrast, CRISPR-Cas9 technology offers a safer, more precise alternative for targeting specific DGK isotypes, minimizing off-target effects.<sup>16</sup> This method, focusing on *ex vivo* T cell engineering, ensures unaffected DGK

### Figure 3. Levels of secreted cytokines following co-culture

Shown are (A) pro-inflammatory/regulatory cytokines, (B) anti-inflammatory cytokines, (C) chemotactic factors, and (D) growth factors in supernatants harvested from unedited T cells (blue) and TAG-72 CAR-T (red) and TAG-72 CAR/DGK $\alpha$ / $\zeta$  KO T cells (purple) co-cultured with the TAG-72<sup>mid</sup> cancer cell line OVCAR-3 for 20 h. Biological and intra-assay triplicates were used and are denoted as mean  $\pm$  SD ( $n = 3$ ). A one-way ANOVA with Tukey's multiple comparison test was used to determine statistical significance. \* $p \leq 0.05$ , \*\* $p \leq 0.01$ , \*\*\* $p \leq 0.001$ , \*\*\*\* $p \leq 0.0001$ .

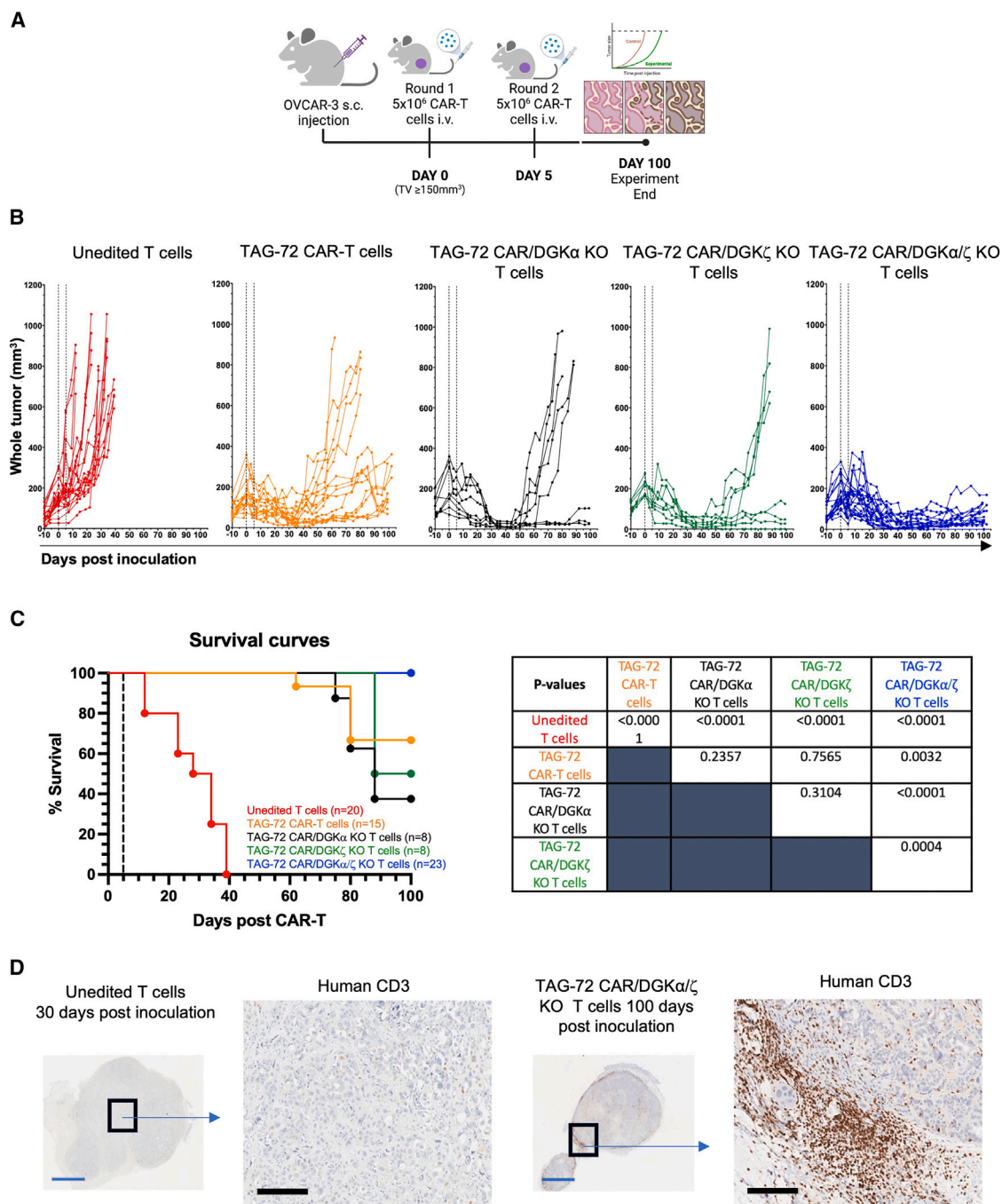


**Figure 4. Impact of CAR-T cells on the *in vivo* growth of established OVCAR-3 tumors**

(A and B) NSG mice bearing OVCAR-3 tumors were treated at 5-day intervals (indicated by dashed lines) with either  $5 \times 10^6$  unedited T cells (red), TAG-72 CAR-T cells (orange), TAG-72 CAR/DGK $\alpha$  single KO T cells (black), TAG-72 CAR/DGK $\zeta$  single KO T cells (green), or TAG-72 CAR/DGK $\alpha/\zeta$  KO T cells (blue) by intravenous (i.v.) injection when the starting tumor volume (STV) was approximately 150 mm<sup>3</sup> in size ( $n = 8-23$  mice per group, results pooled from 5 independent experimental cohorts where animals reached STV size, on average, in 8 weeks). (C) Kaplan-Meier survival curves of all treatment groups. Paired log rank (Mantel-Cox) tests were used to determine statistical significance with probabilities as shown. (D) Representative IHC of OVCAR-3 tumors in NSG xenograft mice. Blue scale bar, 2 mm; black scale bar, 200  $\mu$ m.

activity in other tissues and allows for simultaneous multiple gene edits, providing flexibility for implementing different immunotherapeutic strategies.

The profiling of a large panel of cytokines here demonstrated that the improved cancer reduction and CAR-T cell effectiveness could not be attributed to a single factor. This is not surprising given that deletion of *DGK $\alpha$*  and *DGK $\zeta$*  genes results in an increase in free DAG, which, in turn, can influence a broad spectrum of activation pathways. Indeed, a number of cytokines involved with immune responses are increased. These include those that activate effector cells (for example, *TNF $\alpha$* , *IFN $\gamma$* , and *IL-1 $\beta$* ) and enhance recruitment and *in situ* differentiation (for example, *MIP-1 $\alpha$*  and *MIP-1 $\beta$* , *G-CSF*, *GM-CSF*, and *eotaxin*). They collectively contribute to the improved anti-tumor responses and suggest that, while the CAR-T cells targeting TAG-72 may modulate cytokine levels, the additional *DGK* double-gene deletion further potentiates this effect. Consistent with our findings, previous studies have demonstrated that *DGK* KO in CAR-T cells leads to increased production of pro-inflammatory cytokines, including *IFN $\gamma$*  and *IL-2*, as well as enhanced effector function.<sup>16</sup> Although we did not observe an increase in these specific cytokines, we did note an overall increase in effector function in terms of persistence, suggesting that *DGK* deletion can potentiate the efficacy of CAR-T cells through multiple mechanisms.

The observed increase in *IL-1Ra* levels in both TAG-72 CAR-T cells and TAG-72 CAR/*DGK $\alpha$* / *$\zeta$*  KO T cells suggests that these cells can also enhance the anti-inflammatory response. *IL-1Ra* is a known antagonist of the pro-inflammatory cytokine *IL-1 $\beta$* ,<sup>37</sup> indicating a potential regulatory mechanism that may balance any potential inflammation triggered by CAR-T cell activity. The slight enhancement of *IL-4* may further amplify the anti-inflammatory response by TAG-72 CAR/*DGK $\alpha$* / *$\zeta$*  KO T cells, mitigating rises in pro-inflammatory cytokines. However, while this implies that *DGK* deletion can enhance certain anti-inflammatory responses, its effects may be specific to particular cytokines, like *IL-1Ra*, and less pronounced for others, like *IL-4*. *DGK* deletion may also improve the efficacy of CAR-T cell therapies by boosting immune cell recruitment and activity, although it may also increase the risk of pro-inflammation-related side effects. Our findings also show that TAG-72 CAR-T cells, and particularly TAG-72 CAR/*DGK $\alpha$* / *$\zeta$*  KO T cells, may not only exhibit direct anti-tumor activities but also influence the TME through the secretion of growth factors, such as *PDGF-BB*, *FGF basic*, and *G-CSF*.<sup>32</sup> However, more data are required to confirm these potential effects and the complex interplay of cytokines, chemokines, and growth factors under more relevant conditions (e.g., *in vivo* and in the clinic).

Notably, TAG-72 CAR/*DGK $\alpha$* / *$\zeta$*  KO T cells achieved complete tumor eradication in our xenograft model, with no recurrence up to 100 days post treatment. This indicates that TAG-72 CAR/*DGK $\alpha$* / *$\zeta$*  KO T cells significantly improved tumor control *in vivo* compared to TAG-72 CAR-T cells, potentially due to enhanced T cell killing activity, extended cell longevity, and/or diminished T cell exhaustion. Future studies should elucidate the mechanisms that enhance the cytotox-

icity and persistence of TAG-72 CAR/*DGK $\alpha$* / *$\zeta$*  KO cells to improve clinical application. Moreover, our findings are particularly compelling given the nature of our *in vivo* model. Unlike common approaches that introduce CAR-T cells shortly after tumor cell implantation, simulating a preventive rather than therapeutic scenario, our model challenges CAR-T cells against sizable ( $\geq 150 \text{ mm}^3$ ), well-established tumors. Another study similarly showed that epidermal growth factor receptor variant III (EGFRvIII) CAR-T cells with *DGK $\alpha$* / *$\zeta$*  KO also significantly reduced tumor burden when injected at similarly established tumor volumes, with reduction up to 60 days.<sup>16</sup> Our data, demonstrating dramatic tumor mass reduction under these conditions, not only underscore the potential of our engineered CAR-T cells but also suggest that they may offer significant advantages over current models that may not adequately test therapeutic efficacy against established malignancies. This highlights the importance of adopting more stringent *in vivo* models to better assess the clinical potential of CAR-T cell therapies.

In conclusion, our study characterized and demonstrated the enhanced effectiveness of CRISPR-Cas9-engineered TAG-72 CAR/*DGK $\alpha$* / *$\zeta$*  KO T cells while maintaining a viability and proliferative capacity on par with TAG-72 CAR-T cells. These cells exhibited significant tumor control both *in vitro* and *in vivo*, achieving complete eradication of established tumors *in vivo* without recurrence for up to 100 days, highlighting their potential clinical applicability.

## MATERIALS AND METHODS

### Cell lines

All cell lines were acquired from the American Type Culture Collection (Manassas, VA, USA) and maintained using recommended culture conditions. The OVCAR-3 (HTB-161) ovarian cancer cell line was maintained in RPMI 1640 medium (Sigma-Aldrich, St. Louis, MO, USA) supplemented with 20% (v/v) fetal bovine serum (FBS; Bovogen, Keilor East, VIC, Australia), 0.01 mg/mL bovine insulin (Sigma-Aldrich), and 1  $\times$  penicillin-streptomycin (Pen/Strep; Gibco, Waltham, MA, USA). The ovarian cancer cell line derived from ascites, MES-OV (CRL-3272), was cultured in McCoy's 5A medium (Gibco) containing 10% (v/v) FBS and 1  $\times$  Pen/Strep.

### DNA constructs and lentivirus production

CAR constructs were generated with an scFv for TAG-72 and the lentiviral vectors produced as described previously.<sup>27,38</sup> Following a conventional human secretion signal leader, the scFv was constructed with a 15-residue (G4S)3 linker. The CAR constructs were designed using the hinge and transmembrane regions of human CD8 along with the cytoplasmic signaling domains of 4-1BB and CD3 $\zeta$ . The P2A sequence, a signal sequence directing proteolytic cleavage, was used to direct bicistronic expression of EGFP. A second-generation, self-inactivating bicistronic lentiviral transfer vector was then used to produce the lentiviral vectors for CAR transduction.<sup>39</sup> Briefly, HEK293T cells were plated onto poly-L-lysine-coated tissue culture plates (Sigma-Aldrich). The lentiviral transfer vector DNA, together with packaging and envelope plasmid DNA, was then transfected with Lipofectamine 2000 (Invitrogen, Carlsbad, CA, USA). Viral



supernatant was collected after 48 h and cleared by centrifugation, followed by 0.45- $\mu$ m filtration (Millipore, Burlington, MA, USA). Concentration of lentivirus was performed using a SORVALL Discovery 100 SE ultracentrifuge (90 min at 20,000  $\times$  g; Kendro, Newtown, CT, USA). The resultant virus pellets were resuspended in Dulbecco's PBS (dPBS; Life Technologies, Carlsbad, CA, USA) and stored at  $-80^{\circ}\text{C}$  until use.

### CAR-T cell production

The timeline for production of CAR-T cells is summarized in Figure 1A. Specifically, primary human T cells were isolated from fresh healthy donor whole blood or buffy coat samples obtained from Australian Red Cross Lifeblood (as non-conforming/discarded material not suitable for clinical purposes). All donors provided informed consent prior to collection. The study was conducted in accordance with the Declaration of Helsinki and approved by Monash Health 16055A (Development of Novel Immunotherapies for Cancer, May 10, 2016). From whole-blood samples, peripheral blood mononuclear cells (PBMCs) were isolated by Ficoll-Paque Plus (Cytiva, Buckinghamshire, UK) centrifugation using Leucosep tubes (Greiner Bio-One, Kremsmünster, Austria) as per the manufacturer's instructions. Buffy coat samples were first depleted of red cells via red cell lysis. Isolated PBMCs or lysed buffy coat (LBC) samples were then either used fresh or cryopreserved and thawed prior to use. For activation and transduction, PBMCs or LBCs were thawed (if required), and T cells were isolated using CD4 and CD8 microbeads (Miltenyi Biotec, Bergisch Gladbach, Germany) as per the manufacturer's instructions with an autoMACS Pro (Miltenyi Biotec). Isolated CD4<sup>+</sup> and CD8<sup>+</sup> cells were then activated using TransAct reagent (Miltenyi Biotec) according to the manufacturer's instructions. In brief, cells were incubated with 1/100 dilution of TransAct for a total of  $\sim 72$  h at  $37^{\circ}\text{C}$  and 5%  $\text{CO}_2$  in T cell activation medium (TexMACS medium, Miltenyi Biotec) with 5% (v/v) human AB serum (hAB; Sigma-Aldrich) with IL-2, where, for the first 24 h of activation, 20 IU/mL IL-2 (Miltenyi Biotec) was added. Following the initial 24 h, the T cell suspension was transferred to plates coated with RetroNectin (Takara Bio, Kusatsu, Japan) with lentiviral particles in the presence of 100 IU/mL IL-2. After 72 h, the lentivirus and activation medium were removed via centrifugation, and T cell expansion continued in complete T cell expansion medium comprising IL-2, IL-7, IL-15, IL-21 (Miltenyi Biotec), hAB serum, and Stemulate (Sexton Biotechnologies, Indianapolis, IN, USA) in TexMACS. On day 5 of culture, CRISPR-Cas9 genome editing was performed as outlined below. T cell expansion was continued for up to 14 days. Activated but non-transduced T cells were maintained in parallel for all donors analyzed.

### gRNA and RNP formation

Lentiviral CAR-transduced T cells were washed with dPBS for Cas9 ribonucleoprotein (RNP) nucleofection. CRISPR RNAs (crRNAs) and *trans*-activating crRNAs (Synthego, Redwood City, CA, USA or Integrated DNA Technologies, Coralville, IA, USA) were annealed to form the full-length gRNAs as described previously.<sup>16,40</sup> Cas9 RNPs were prepared before transfection by incubating Cas9 protein

with the full-length gRNAs at a 1:2 ratio at room temperature for 10–20 min. To transfect the Cas9 RNP, T cells were electroporated using the 4D-Nucleofector device (Lonza, Basel, Switzerland). Two days after T cell activation was the time point used to verify gRNA in activated T cells in preliminary experiments. To generate gene KO CAR-T cells, RNP nucleofection was performed on day 5 of culture.

### CRISPR indel analysis

The efficacy and mutation spectrum of CRISPR-Cas9 genome editing was analyzed by the Inference of CRISPR Edits (ICE) assay.<sup>41</sup> The total indel frequency reflects the editing efficiency (percentage of the edited sample with a non-wild-type sequence); it is determined by comparing the edited trace to the control trace. The KO frequency is the proportion of cells with either a frameshift or 21+ bp indel, likely to result in a functional KO of the targeted gene. Genomic DNA was extracted from cells 4 days after electroporation using the NucleoSpin Blood DNA Mini Kit (Macherey-Nagel, Düren, Germany) according to manufacturer's instructions. Polymerase chain reaction (PCR) amplicons spanning the gRNA genomic target sites were generated using Q5 High-Fidelity DNA polymerase (New England Biolabs, Ipswich, MA, USA). For analyzing genetic modification frequencies using ICE, the purified PCR products were Sanger sequenced and the sequence chromatograms analyzed using the online Synthego ICE Analysis tool (<https://ice.synthego.com/#/>).

### Western blot

Edited T cell pellets were lysed in radio-immunoprecipitation assay (buffer (Sigma-Aldrich) with a protease inhibitor cocktail (Roche, Basel, Switzerland) on ice for 10 min. After centrifugation at 10,000  $\times$  g for 10 min at  $4^{\circ}\text{C}$ , the lysates were separated by Mini-PROTEAN TGX precast gels (Bio-Rad Laboratories, Hercules, CA, USA) and transferred to a polyvinylidene difluoride membrane (Millipore) using the Mini-PROTEAN Tetra Cell system (Bio-Rad) according to the manufacturer's instructions. Antibodies against DGK $\alpha$  (Santa Cruz Biotechnology, Dallas, TX, USA) and DGK $\zeta$  (Sigma-Aldrich) were used as probes. Immune complexes were detected using IRDye secondary antibodies and the Odyssey Imaging system (LI-COR Biosciences, Lincoln, NE, USA).

### Flow cytometry

Transduction efficiency was evaluated at least 11 days following transduction by flow cytometry using either GFP or goat anti-mouse F(ab')<sub>2</sub> allophycocyanin (APC; Jackson ImmunoResearch Laboratories, West Grove, PA, USA) or anti-FLAG M2-fluorescein isothiocyanate (Sigma-Aldrich). The frequency of T cell subsets was determined by staining for CD3 phycoerythrin (PE; clone REA613), CD4 VioBlue (clone VIT4), CD8 VioGreen (clone BW135-80), CCR7 PE-Vio770 (clone REA675), and CD45RO APC (clone REA611). T cell activation was characterized by staining for histocompatibility leukocyte antigen-DR PE-Vio615 (clone REA805) and CD137 APC (clone REA765). All antibodies were acquired from Miltenyi Biotec (Bergisch Gladbach, Germany) unless stated otherwise. Staining was performed at  $4^{\circ}\text{C}$  for 15–30 min. Cells were then washed with 3% (v/v) FBS in dPBS. Either Viability

405/520 dye (Miltenyi Biotec) or propidium iodide (Sigma-Aldrich) was used to select for viable cells. Data were acquired using the MACSQuant analyzer 10 (Miltenyi Biotec), and analysis was subsequently performed using FlowLogic software (Inivai Technologies, Mentone, VIC, Australia).

### ***In vitro* T cell cytotoxicity assay**

The real-time cell analysis instrument xCELLigence (ACEA Biosciences, San Diego, CA, USA) was utilized for the assessment of T cell function *in vitro*. Before use, effector cells were transferred to fresh T cell expansion medium or activation medium comprising 200 IU/mL IL-2 or recovery medium comprising IL-7 in basal medium for 12–24 h. In this instance, basal medium refers to TexMACS supplemented with 5% (v/v) hAB serum. T cells were co-cultured with cancer cell lines at an effector to target ratio (E:T) of 5:1 unless stated otherwise. Target cells were plated for 6–24 h in 96-well electronic microtiter plates (ACEA Biosciences) before addition of effector cells. Cell impedance was monitored at 15-min intervals for 20 h from addition of effector cells. All data were normalized to the time of addition of effector cells unless stated otherwise and are presented here as the arbitrary unit-normalized cell index (CI). CAR-T cell function was calculated as % cytotoxicity =  $([\text{normalized CI}_{\text{target cells alone}} - \text{normalized CI}_{\text{test}}] / \text{normalized CI}_{\text{target cells alone}}) \times 100$ .

### **Cytokine array**

Supernatant samples from T cell functional assays were retained following 20-h co-culture and frozen at  $-80^{\circ}\text{C}$  until required. Supernatants were subsequently analyzed for secreted human cytokines using the Bio-Plex Pro Human Cytokine 27-plex Assay according to the manufacturer's instructions (Bio-Rad). Plates were read using the Bio-Plex MAGPIX system (Bio-Rad). Data were acquired using Bio-Plex Manager MP software and processed using Bio-Plex Data Pro Plus (both from Bio-Rad).

### ***In vivo* tumor studies**

All animal experiments were pre-approved by the Monash Medical Centre Animal Ethics Committee (MMCA/2016/61 and MMCA/2018/04), and all procedures followed the National Health and Medical Research Council of Australia guidelines for the use and care of experimental animals. *In vivo* models were established using female 6- to 12-week-old NSG mice purchased from Australian BioResources or bred from in-house colonies (Monash Animal Research Platform). OVCAR-3 cells ( $1 \times 10^7$ ) were prepared in 100  $\mu\text{L}$  of PBS combined with an equal volume of Matrigel (Corning Life Sciences, Corning, NY, USA) and injected s.c. into the back flank. OVCAR-3 tumors were allowed to reach approximately 150  $\text{mm}^3$  in size before treatment was commenced; on average, this was approximately 8 weeks. Mice were randomized into experimental groups, and two injections of  $5 \times 10^6$  CAR<sup>+</sup> T cells/injection were administered intravenously (i.v.) at 5-day intervals (day 0 and day 5; Figure 4A). Control mice received unedited T cells at comparable dosages. Tumor volume and clinical parameters of animal health were monitored regularly until the experiment end (day 100 following initial CAR-T

cell treatment or tumor volume  $> 1,000 \text{ mm}^3$ ). Tumors were measured using digital calipers, and volumes were calculated using:  $(\text{length} \times \text{width} \times \text{width})/2 \text{ (mm}^3\text{)}$ . At the end of experiments, mice were euthanized by  $\text{CO}_2$  inhalation.

### **IHC**

S.c. OVCAR-3 tumors from NSG xenograft mice were collected post euthanasia and immediately fixed in 4% paraformaldehyde (Sigma-Aldrich), and then IHC was performed by the Monash Histology Platform (Clayton, VIC, Australia). In brief, formalin-fixed and paraffin-embedded 4- $\mu\text{m}$  longitudinal sections were stained with primary antibodies against human-specific TAG-72 (B72.3; Abcam, Cambridge, UK) and CD3 (F7.2.38, Abcam) alongside hematoxylin and eosin counterstains using a Dako PT Link and Autostainer (Agilent Technologies, Santa Clara, CA, USA). Images were captured using the Aperio ScanScope AT Turbo digital slide scanner and associated ImageScope 12.1 software (both from Leica Biosystems, Wetzlar, Germany).

### **Statistical analysis**

Data represent mean  $\pm$  SD from at least three biological replicates unless stated otherwise. GraphPad Prism 10 software (GraphPad, Boston, MA, USA) was used to perform statistical analysis throughout. Results were analyzed using a Kruskal-Wallis non-parametric test, one-way ANOVA with Tukey's multiple comparison test, or log rank (Mantel-Cox) test as indicated. Statistical significance was defined as  $p \leq 0.05$  ( $*p \leq 0.05$ ,  $**p \leq 0.01$ ,  $***p \leq 0.001$ , and  $****p \leq 0.0001$ ).

### **DATA AVAILABILITY**

The raw data supporting the conclusions of this article will be made available by the authors upon request.

### **ACKNOWLEDGMENTS**

We acknowledge the use of the facilities and equipment and technical assistance of the Monash Histology Platform, Department of Anatomy and Developmental Biology, Monash Health Translation Precinct Cell Therapy and Regenerative Medicine Platform, FlowCore, Monash Animal Research Platform and Monash Medical Centre Animal Facility (all at Monash University). We also thank Drs. Michael Kershaw, Ian Nisbet, Maureen Howard, and Walid Azar for scientific feedback, invaluable guidance, and ongoing critique of this study. Additionally, we thank Dr. Thao Nguyen and Callum Docherty for technical support. Figures 1A and 4A were created with BioRender. The research described in this paper was funded by Cartherics Pty Ltd.

### **AUTHOR CONTRIBUTIONS**

Conceptualization, R.S., R.L.B., A.O.T., V.J.E., M.V.H., N.-Y.N.N., J.Y.L., S.K., and P.J.H.; methodology, V.J.E., M.V.H., N.-Y.N.N., J.Z., J.Y.L., and R.S.; formal analysis and data curation, V.J.E., M.V.H., N.-Y.N.N., J.Z., R.S., R.L.B., and A.P.; writing – original draft, V.J.E., M.V.H., N.-Y.N.N., R.S., R.L.B., and A.P.; writing – review and editing, V.J.E., M.V.H., N.-Y.N.N., R.S., R.L.B., A.P., J.Y.L., and A.O.T.; supervision, R.S., R.L.B., and A.O.T.; project administration, V.J.E., R.S., M.V.H., N.-Y.N.N., J.Y.L., and S.K. All authors have read and agreed to the published version of the manuscript.

### **DECLARATION OF INTERESTS**

At the time of this work being conducted, all authors, except for P.J.H., J.Y.L., and S.K., were paid employees of Cartherics and currently hold options and/or equity in the company. R.L.B. and A.O.T. are key Cartherics executives. P.J.H. and R.S. are currently

Cartherics consultants. R.L.B., A.O.T., V.J.E., and R.S. are inventors on Cartherics-owned patent applications related to this work. J.Y.L. and S.K. are employees of ToolGen Inc.

## REFERENCES

- Halim, L., and Maher, J. (2020). CAR T-cell immunotherapy of B-cell malignancy: the story so far. *Ther. Adv. Vaccines Immunother.* 8, 2515135520927164.
- Marofi, F., Motavalli, R., Safonov, V.A., Thangavelu, L., Yumashev, A.V., Alexander, M., Shomali, N., Chartrand, M.S., Pathak, Y., Jarahian, M., et al. (2021). CAR T cells in solid tumors: challenges and opportunities. *Stem Cell Res. Ther.* 12, 81.
- Martinez, M., and Moon, E.K. (2019). CAR T Cells for Solid Tumors: New Strategies for Finding, Infiltrating, and Surviving in the Tumor Microenvironment. *Front. Immunol.* 10, 128.
- Rupp, L.J., Schumann, K., Roybal, K.T., Gate, R.E., Ye, C.J., Lim, W.A., and Marson, A. (2017). CRISPR/Cas9-mediated PD-1 disruption enhances anti-tumor efficacy of human chimeric antigen receptor T cells. *Sci. Rep.* 7, 737.
- Menger, L., Sledzinska, A., Bergerhoff, K., Vargas, F.A., Smith, J., Poirat, L., Pule, M., Hererro, J., Peggs, K.S., and Quezada, S.A. (2016). TALEN-Mediated Inactivation of PD-1 in Tumor-Reactive Lymphocytes Promotes Intratumoral T-cell Persistence and Rejection of Established Tumors. *Cancer Res.* 76, 2087–2093.
- McGowan, E., Lin, Q., Ma, G., Yin, H., Chen, S., and Lin, Y. (2020). PD-1 disrupted CAR-T cells in the treatment of solid tumors: Promises and challenges. *Biomed. Pharmacother.* 121, 109625.
- Dimitri, A., Herbst, F., and Fraietta, J.A. (2022). Engineering the next-generation of CAR T-cells with CRISPR-Cas9 gene editing. *Mol. Cancer* 21, 78.
- Khan, A., and Sarkar, E. (2022). CRISPR/Cas9 encouraged CAR-T cell immunotherapy reporting efficient and safe clinical results towards cancer. *Cancer Treat. Res. Commun.* 33, 100641.
- Kanoh, H., Yamada, K., and Sakane, F. (1990). Diacylglycerol kinase: a key modulator of signal transduction? *Trends Biochem. Sci.* 15, 47–50.
- Baldanzi, G., Pighini, A., Bettio, V., Rainero, E., Traini, S., Chianale, F., Porporato, P.E., Filigheddu, N., Mesturini, R., Song, S., et al. (2011). SAP-mediated inhibition of diacylglycerol kinase  $\alpha$  regulates TCR-induced diacylglycerol signaling. *J. Immunol.* 187, 5941–5951.
- Noessner, E. (2017). DGK- $\alpha$ : A Checkpoint in Cancer-Mediated Immuno-Inhibition and Target for Immunotherapy. *Front. Cell Dev. Biol.* 5, 16.
- Zha, Y., Marks, R., Ho, A.W., Peterson, A.C., Janardhan, S., Janardhan, S., Brown, I., Praveen, K., Stang, S., Stone, J.C., and Gajewski, T.F. (2006). T cell anergy is reversed by active Ras and is regulated by diacylglycerol kinase- $\alpha$ . *Nat. Immunol.* 7, 1166–1173.
- Olenchok, B.A., Guo, R., Carpenter, J.H., Jordan, M., Topham, M.K., Koretzky, G.A., and Zhong, X.P. (2006). Disruption of diacylglycerol metabolism impairs the induction of T cell anergy. *Nat. Immunol.* 7, 1174–1181.
- Moon, E.K., Wang, L.C., Dolfi, D.V., Wilson, C.B., Ranganathan, R., Sun, J., Kapoor, V., Scholler, J., Puré, E., Milone, M.C., et al. (2014). Multifactorial T-cell hypofunction that is reversible can limit the efficacy of chimeric antigen receptor-transduced human T cells in solid tumors. *Clin. Cancer Res.* 20, 4262–4273.
- Joshi, R.P., Schmidt, A.M., Das, J., Pytel, D., Riese, M.J., Lester, M., Diehl, J.A., Behrens, E.M., Kambayashi, T., and Koretzky, G.A. (2013). The zeta isoform of diacylglycerol kinase plays a predominant role in regulatory T cell development and TCR-mediated ras signaling. *Sci. Signal.* 6, ra102.
- Jung, I.Y., Kim, Y.Y., Yu, H.S., Lee, M., Kim, S., and Lee, J. (2018). CRISPR/Cas9-Mediated Knockout of DGK Improves Antitumor Activities of Human T Cells. *Cancer Res.* 78, 4692–4703.
- Sullivan, L.B., Gui, D.Y., and Vander Heiden, M.G. (2016). Altered metabolite levels in cancer: implications for tumour biology and cancer therapy. *Nat. Rev. Cancer* 16, 680–693.
- Li, J., Pan, C., Boese, A.C., Kang, J., Umamo, A.D., Magliocca, K.R., Yang, W., Zhang, Y., Lonial, S., Jin, L., and Kang, S. (2020). DGKA Provides Platinum Resistance in Ovarian Cancer Through Activation of c-JUN-WEE1 Signaling. *Clin. Cancer Res.* 26, 3843–3855.
- Wu, J.W.Y., Dand, S., Doig, L., Papenfuss, A.T., Scott, C.L., Ho, G., and Ooi, J.D. (2021). T-Cell Receptor Therapy in the Treatment of Ovarian Cancer: A Mini Review. *Front. Immunol.* 12, 672502.
- Matulonis, U.A., Sood, A.K., Fallowfield, L., Howitt, B.E., Sehoul, J., and Karlan, B.Y. (2016). Ovarian cancer. *Nat. Rev. Dis. Primers* 25, 16061. <https://doi.org/10.1038/nrdp.2016.61>.
- Thor, A., Viglione, M.J., Muraro, R., Ohuchi, N., Schlom, J., and Gorstein, F. (1987). Monoclonal antibody B72.3 reactivity with human endometrium: a study of normal and malignant tissues. *Int. J. Gynecol. Pathol.* 6, 235–247.
- Johnson, V.G., Schlom, J., Paterson, A.J., Bennett, J., Magnani, J.L., and Colcher, D. (1986). Analysis of a human tumor-associated glycoprotein (TAG-72) identified by monoclonal antibody B72.3. *Cancer Res.* 46, 850–857.
- Genega, E.M., Hutchinson, B., Reuter, V.E., and Gaudin, P.B. (2000). Immunophenotype of high-grade prostatic adenocarcinoma and urothelial carcinoma. *Mod. Pathol.* 13, 1186–1191.
- Scott, A.M., Akhurst, T., Lee, F.T., Ciprotti, M., Davis, I.D., Weickhardt, A.J., Gan, H.K., Hicks, R.J., Lee, S.T., Kocovski, P., et al. (2020). First clinical study of a pegylated diabody (124)I-labeled PEG-AVP0458 in patients with tumor-associated glycoprotein 72 positive cancers. *Theranostics* 10, 11404–11415.
- Chauhan, S.C., Vinayek, N., Maher, D.M., Bell, M.C., Dunham, K.A., Koch, M.D., Lio, Y., and Jaggi, M. (2007). Combined staining of TAG-72, MUC1, and CA125 improves labeling sensitivity in ovarian cancer: antigens for multi-targeted antibody-guided therapy. *J. Histochem. Cytochem.* 55, 867–875.
- Ponnusamy, M.P., Venkatraman, G., Singh, A.P., Chauhan, S.C., Johansson, S.L., Jain, M., Smith, L., Davis, J.S., Remmenga, S.W., and Batra, S.K. (2007). Expression of TAG-72 in ovarian cancer and its correlation with tumor stage and patient prognosis. *Cancer Lett.* 251, 247–257.
- Shu, R., Evtimov, V.J., Hammett, M.V., Nguyen, N.Y.N., Zhuang, J., Hudson, P.J., Howard, M.C., Pupovac, A., Trounson, A.O., and Boyd, R.L. (2021). Engineered CAR-T cells targeting TAG-72 and CD47 in ovarian cancer. *Mol. Ther. Oncolytics* 20, 325–341.
- Murad, J.P., Kozłowska, A.K., Lee, H.J., Ramamurthy, M., Chang, W.C., Yazaki, P., Colcher, D., Shively, J., Cristea, M., Forman, S.J., and Priceman, S.J. (2018). Effective Targeting of TAG72(+) Peritoneal Ovarian Tumors via Regional Delivery of CAR-Engineered T Cells. *Front. Immunol.* 9, 2268.
- Menten, P., Wuyts, A., and Van Damme, J. (2002). Macrophage inflammatory protein-1. *Cytokine Growth Factor Rev.* 13, 455–481.
- Shibuya, M. (2011). Vascular Endothelial Growth Factor (VEGF) and Its Receptor (VEGFR) Signaling in Angiogenesis: A Crucial Target for Anti- and Pro-Angiogenic Therapies. *Genes Cancer* 2, 1097–1105.
- Kim, H.J., and Jung, Y. (2020). The Emerging Role of Eosinophils as Multifunctional Leukocytes in Health and Disease. *Immune Netw.* 20, e24.
- Zhao, H., Wu, L., Yan, G., Chen, Y., Zhou, M., Wu, Y., and Li, Y. (2021). Inflammation and tumor progression: signaling pathways and targeted intervention. *Signal Transduct. Target. Ther.* 6, 263.
- Hege, K.M., Bergsland, E.K., Fisher, G.A., Nemunaitis, J.J., Warren, R.S., McArthur, J.G., Lin, A.A., Schlom, J., June, C.H., and Sherwin, S.A. (2017). Safety, tumor trafficking and immunogenicity of chimeric antigen receptor (CAR)-T cells specific for TAG-72 in colorectal cancer. *J. Immunother. Cancer* 5, 22.
- Krishna, S., and Zhong, X. (2013). Role of diacylglycerol kinases in T cell development and function. *Crit. Rev. Immunol.* 33, 97–118.
- Gu, J., Wang, C., Cao, C., Huang, J., Holzhauser, S., Desilva, H., Wesley, E.M., Evans, D.B., Benci, J., Wichroski, M., et al. (2021). DGKzeta exerts greater control than DGKalpha over CD8(+) T cell activity and tumor inhibition. *Oncol Immunology* 10, 1941566.
- Riese, M.J., Moon, E.K., Johnson, B.D., and Albelda, S.M. (2016). Diacylglycerol Kinases (DGKs): Novel Targets for Improving T Cell Activity in Cancer. *Front. Cell Dev. Biol.* 4, 108.
- Rider, P., Carmi, Y., Yossef, R., Guttman, O., Eini, H., Azam, T., Dinarello, C.A., and Lewis, E.C. (2015). IL-1 Receptor Antagonist Chimeric Protein: Context-Specific and Inflammation-Restricted Activation. *J. Immunol.* 195, 1705–1712.

38. Shu, R., Hammett, M., Evtimov, V., Pupovac, A., Nguyen, N.Y., Islam, R., Zhuang, J., Lee, S., Kang, T.H., Lee, K., et al. (2023). Engineering T cell receptor fusion proteins using nonviral CRISPR/Cas9 genome editing for cancer immunotherapy. *Bioeng. Transl. Med.* 8, e10571.
39. Shu, R., Wong, W., Ma, Q.-H., Yang, Z.Z., Zhu, H., Liu, F.J., Wang, P., Ma, J., Yan, S., Polo, J.M., et al. (2015). APP intracellular domain acts as a transcriptional regulator of miR-663 suppressing neuronal differentiation. *Cell Death Dis.* 6, e1651.
40. Boyd, N., Trounson, A.O., Cao, H., Tiedemann, M.J., Boyd, R., Shu, R., and Calhabeu, F.L. (2022). Methods and compositions for generating stem cell-derived immune cells with enhanced function, PCT/AU2022/050075. WO2022170384 WO2022.
41. Conant, D., Hsiau, T., Rossi, N., Oki, J., Maures, T., Waite, K., Yang, J., Joshi, S., Kelso, R., Holden, K., et al. (2022). Inference of CRISPR Edits from Sanger Trace Data. *CRISPR J.* 5, 123–130.